

Extension of Bandstop Filter Topology With Inter-Resonator Coupling Structures to Higher-Order Filters

Tae-Hak Lee, *Student Member, IEEE*, Chang-Soo Ahn, Young-Sik Kim, *Member, IEEE*, and Juseop Lee, *Member, IEEE*

Abstract—This letter presents a rigorous extension of the concept for the bandstop filter (BSF) with inter-resonator couplings to a higher order filter. We show that a BSF topology with inter-resonator couplings can exhibit the frequency response that a conventional BSF topology without inter-resonator couplings generates. Equivalence between the coupling matrices of the two topologies are shown. As an example, this letter shows that fourth-order BSFs with and without inter-resonator couplings can exhibit identical frequency responses.

Index Terms—Bandstop filter (BSF), filter synthesis, substrate integrated resonator filter.

I. INTRODUCTION

IN modern communication systems, a capacity covering one or more functions leads to the improvement of a front-end's component. It is inevitable to achieve tunable or switchable characteristics for filters. Therefore, many types of tunable filters have been proposed [1]–[3]. In [1], coupled lines are utilized for tunable characteristics, and a Barium-Strontium-Titanate (BST) varactors or thermal actuators placed in the ground plane are used to achieve the variable center frequencies [2], [3]. In these tunable filters, each resonator is coupled to a microstrip line, not coupled each other. Unlike these conventional Bandstop filter (BSF) structures, BSF topologies containing inter-resonator couplings have been proposed to achieve switchable characteristics [4]–[7]. Existence of the inter-resonator coupling structure allows for achieving the switchable characteristics between bandstop and bandpass or all-pass. Most filter topologies are limited to the second-order structure. This letter presents a way to extend the BSF topology with inter-resonator coupling(s) to a higher-order filter design by showing a fourth-order BSF topology. In addition, we show that the presented BSF topology can be synthesized in such a way that it exhibits the same frequency response the conventional BSF generates. The novelty of this letter is that, for the first time, shows the relationship between the BSF topologies with and without inter-

resonator couplings. Using the relationship, this letter shows how to extract the coupling matrix of the topology with inter-resonator couplings. Since no complicated math is used, this method for extracting the coupling matrix can find its practical applications.

II. THEORY

Fig. 1 shows a low-pass circuit topology for the fourth-order conventional BSF and its coupling matrix while the proposed circuit topology and coupling matrix are shown in Fig. 2. In Figs. 1(a) and 2(a), the numbers represent the resonators which are modeled as a unit capacitor in parallel with constant $jM_{i,i}$ ($i = 1, 2, 3,$ and 4) to account for the frequency shift of the resonant frequency, and NRN means non-resonating-node which is connected to the ground by a constant reactance, $jB_{N,i}$ ($i = 1$ and 2) [8]. All nodes (source, load, resonators, and NRNs) are connected by admittance inverters whose values are represented by $jM_{p,q}$ ($p, q = 1, 2, 3, 4, N1$ and $N2$), and the connections between the nodes are represented using solid lines. Fig. 1(a) shows a conventional BSF topology which does not possess couplings between resonators whereas the couplings between resonators are included in the BSF topology as shown in Fig. 2(a). Two coupling matrices for two topologies are shown in Figs. 1(b) and 2(b). The unprimed and primed coupling coefficients of each matrix correspond to the topologies shown in Figs. 1(a) and 2(a), respectively. The reflected and transmitted power ratios can be found from the coupling matrices, and we can derive the equivalence between the two topologies by comparing the expressions for the reflected and transmitted power ratios of the one topology with those of the other topology. It has been found that the conventional and new topologies exhibit the same frequency response given that

$$\begin{aligned}
 M'_{S,1} &= M'_{4,L} = M_{2,N1} (= M_{N2,3}) \\
 M'_{2,N1} &= M'_{N2,3} = M_{S,1} (= M_{4,1}) \\
 M'_{1,2} &= M'_{3,4} = M_{S,1} M_{2,N1} (= M_{N2,3} M_{4,L}) \\
 M'_{1,1} &= -M'_{4,4} = \pm M_{2,2} = \mp M_{3,3} \\
 M'_{2,2} &= -M'_{3,3} = \pm M_{1,1} = \mp M_{4,4}. \quad (1)
 \end{aligned}$$

With the help of the relationship between two coupling matrices, all coupling coefficients of the topology which has inter-resonator couplings can be found from the values of the coupling coefficients of the conventional one by using (1). Hence, the BSF with the inter-resonator couplings can be conveniently synthesized by synthesizing the conventional BSF. For example, the coupling coefficients of two topologies

Manuscript received March 18, 2013; revised May 20, 2013; accepted May 21, 2013. Date of publication July 15, 2013; date of current version August 05, 2013. This work was supported by the Agency for Defense Development under UD120046FD.

T.-H. Lee, Y.-S. Kim, and J. Lee are with the Department of Radio Communications Engineering, Korea University, Seoul, Korea (e-mail: ifsnow@iee.org).

C.-S. Ahn is with the Third. R&D Institute-2, Agency for Defence Development, Daejeon, Korea.

Color versions of one or more of the figures in this letter are available online at <http://ieeexplore.ieee.org>.

Digital Object Identifier 10.1109/LMWC.2013.2269217

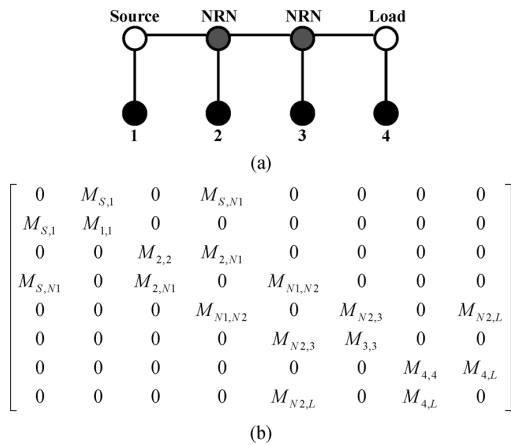


Fig. 1. Conventional fourth-order BSF without inter-resonator coupling (a) coupling routing diagram, (b) coupling matrix.

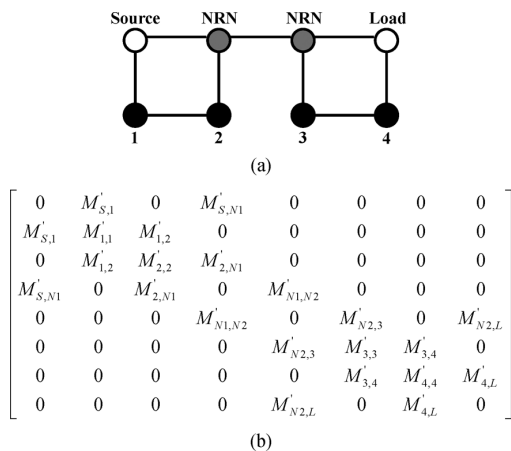


Fig. 2. Fourth-order BSF with inter-resonator coupling (a) coupling routing diagram, (b) coupling matrix.

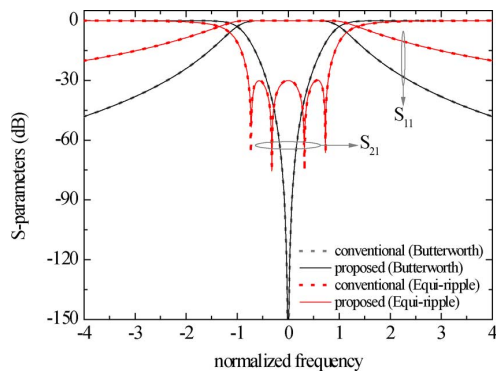


Fig. 3. Frequency responses from the BSF with and without inter-resonator couplings.

for the Butterworth response are given in Table I. The coupling coefficients, $M_{N1,N2}$ and $M'_{N1,N2}$, can be either ± 1 . A different frequency response such as 30 dB equi-ripple response can also be obtained with non-zero value of $M_{i,i}$ ($i = 1, 2, 3$ and 4). The softer slope of S_{11} of the equi-ripple response in the passband is due to the complex reflection zeros. The coupling coefficients for the equi-ripple response are listed in Table II for the two BSF topologies. Solid and dotted lines in Fig. 3 show the frequency responses of the BSF topologies with and without inter-resonator couplings, respectively. The indistinguishable frequency responses verify (1).

TABLE I
COUPLING COEFFICIENTS FOR BUTTERWORTH BSF

$M_{S,1}$	$M_{2,N1}$	$M_{1,2}$	$M_{S,N1}$	$M_{1,1}$	$M_{2,2}$
$M_{4,L}$	$M_{N2,3}$	$M_{3,4}$	$M_{N2,L}$	$-M_{4,4}$	$-M_{3,3}$
0.875	1.359	0.000	1.000	0.000	0.000
$M'_{S,1}$	$M'_{2,N1}$	$M'_{1,2}$	$M'_{S,N1}$	$M'_{1,1}$	$M'_{2,2}$
$M'_{4,L}$	$M'_{N2,3}$	$M'_{3,4}$	$M'_{N2,L}$	$-M'_{4,4}$	$-M'_{3,3}$
1.359	0.875	1.189	1.000	0.000	0.000

TABLE II
COUPLING COEFFICIENTS FOR A 30 dB EQUI-RIPPLE BSF

$M_{S,1}$	$M_{2,N1}$	$M_{1,2}$	$M_{S,N1}$	$M_{1,1}$	$M_{2,2}$
$M_{4,L}$	$M_{N2,3}$	$M_{3,4}$	$M_{N2,L}$	$-M_{4,4}$	$-M_{3,3}$
0.875	1.359	0.000	1.000	0.321	-0.729
$M'_{S,1}$	$M'_{2,N1}$	$M'_{1,2}$	$M'_{S,N1}$	$M'_{1,1}$	$M'_{2,2}$
$M'_{4,L}$	$M'_{N2,3}$	$M'_{3,4}$	$M'_{N2,L}$	$-M'_{4,4}$	$-M'_{3,3}$
1.359	0.875	1.189	1.000	-0.729	0.321

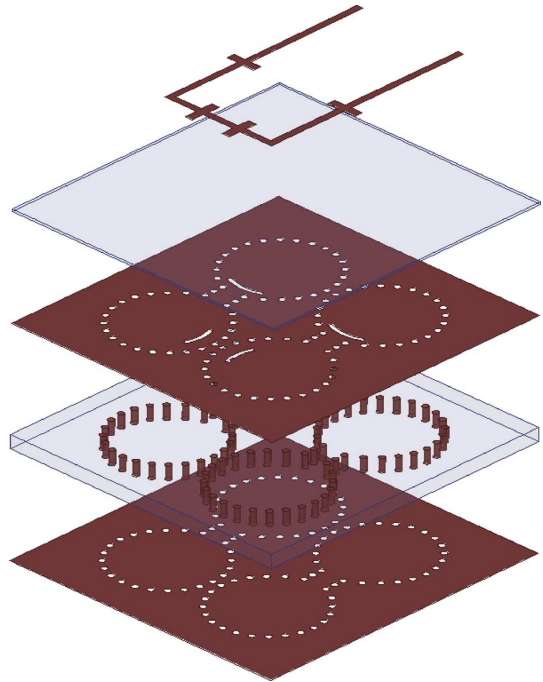


Fig. 4. Layer-by-layer expanded view of the fourth-order BSF with inter-resonator couplings.

III. EXPERIMENTAL RESULTS

To verify the relationship between the two topologies, two BSFs with each topology are designed and fabricated. Both BSFs consist of two layers. The upper layer contains a microstrip line used to couple to the resonators, and four substrate-integrated cavity type resonators exist in the bottom layer. For the upper layer, a RO5880 substrate which has 0.508 mm thickness and 2.2 dielectric constant is used, and a TMM3 substrate having 3.175 mm thickness and 3.27 dielectric constant is used for the bottom layer. Fig. 4 shows layer-by-layer drawing of the BSF with the inter-resonator couplings. However, the detailed physical structure for the BSF with the conventional topology is not shown here due to the limited space, but the fabricated structure will be shown later. As can be seen in Fig. 4, magnetic couplings between the microstrip line and cavity are made through four coupling slots placed on

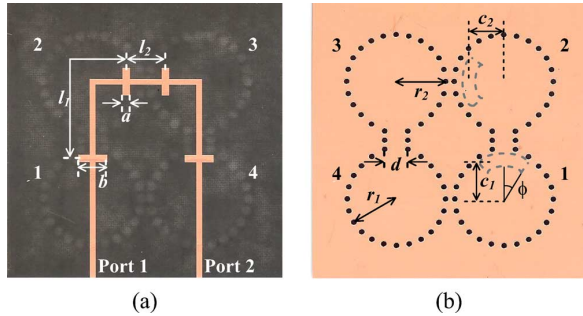


Fig. 5. Photograph of the fabricated fourth-order BSF with inter-resonator couplings. $a = 2$, $b = 7.56$, $l_1 = 29.8$, $l_2 = 10.2$, $r_1 = 12.9$, $r_2 = 13$, $d = 3$, $c_1 = 11$, $c_2 = 8.8$, $\phi = 25^\circ$. All dimensions are in millimeters.

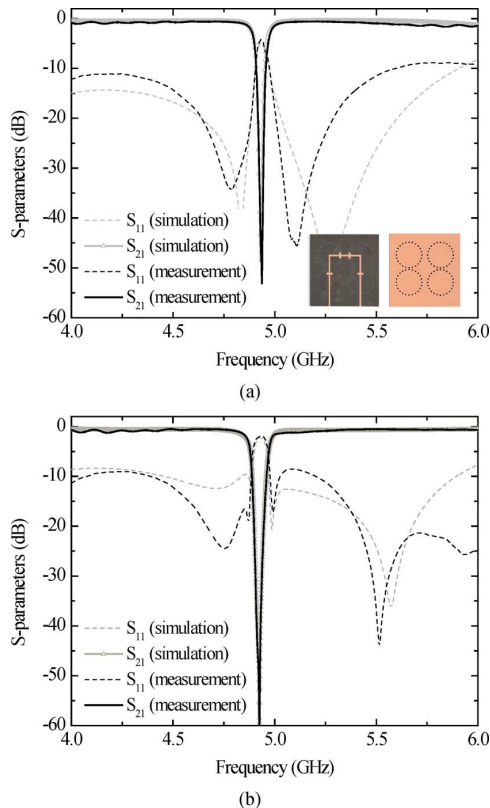


Fig. 6. (a) Simulation and measurement results of conventional BSF, (b) simulation and measurement results of proposed BSF.

the top side of the cavity. Four rectangular-shaped capacitive patches are placed just above the coupling slots for achieving a good return loss performance [9]. The lengths between coupling slots, l_1 and l_2 , are 270° and 90° at the center frequency. Each of the inter-resonator couplings between resonators 1 and 2, and resonators 3 and 4 is established using an inductive iris. It can be modeled as a shunt inductor which generates $+90$ degree phase shift. The coupling coefficients which represent the inter-resonator couplings are positive numbers as shown in Tables I and II. Since $M_{S,N1}$ and $M_{N2,L}$ are also positive numbers, the $3/4$ wavelength transmission lines are used for generating $+90$ degree phase shift. Since $M_{N1,N2}$ can be either positive or negative, the transmission line between resonators 2 and 3 can be either $1/4$ or $3/4$ wavelength long. For minimizing the loss, a $1/4$ wavelength transmission line is used between

resonators 2 and 3. Two fourth-order BSFs are designed with target frequency of 4.9 GHz and 100 MHz bandwidth and the detailed dimensions are shown in Fig. 5 for the case of the BSF with inter-resonator coupling structure. All dimensions are determined to meet the relationship between the coupling coefficients, k , and the normalized coupling coefficients, M , following a well-known design procedure [10]. In Fig. 6, the simulation and measurement results of two fabricated BSF are shown and good agreement between the two responses can be found, obtaining a Butterworth-type response. Both BSFs achieve about 50 dB rejection level in the stopband. The insertion losses and reflection coefficients in the passband are less than about 1.5 dB and -10 dB, respectively. The return loss in the passband region can be improved by more careful design of the coupling patches [9]. Two photographs of fabricated conventional BSF which does not possess the inter-resonator coupling structures can be found as an inset of Fig. 6(a). This indicates that the filter topology with the coupling coefficients satisfying (1) can replicate the frequency response generated by the conventional filter topology.

IV. CONCLUSION

This letter presented a rigorous extension of the concept for the BSF with the inter-resonator couplings to a higher order filter. It also showed an analytic synthesis method for the BSF topology with the inter-resonator coupling structures. It showed that the coupling matrix of the BSF topology with the inter-resonator coupling structures can be obtained directly from that of the conventional BSF topology which does not contain the inter-resonator couplings. Measurement verified that the BSF topology with the inter-resonator couplings can exhibit the frequency responses that the conventional BSF topology generates.

REFERENCES

- [1] D. Auffray and J. L. Lacombe, "Electronically tunable band-stop filter," in *IEEE MTT-S Int. Dig.*, 1988, pp. 439–442.
- [2] Y.-H. Chun, J.-S. Hong, T. J. Jackson, P. Bao, and M. J. Lancaster, "BST varactor tuned bandstop filter with slotted ground structure," in *IEEE MTT-S Int. Dig.*, 2008, pp. 1115–1118.
- [3] W. D. Yan and R. R. Mansour, "Compact tunable bandstop filter integrated with large deflected actuators," in *IEEE MTT-S Int. Dig.*, 2007, pp. 1611–1614.
- [4] J. Lee, E. Naglich, H. H. Sigmarsson, D. Peroulis, and W. Chappell, "New bandstop filter circuit topology and its application to design of a bandstop-to-bandpass switchable filter," *IEEE Trans. Microw. Theory Tech.*, vol. 61, no. 3, pp. 1114–1123, Mar. 2013.
- [5] J. Lee, E. J. Naglich, and W. J. Chappell, "Frequency response control in frequency-tunable bandstop filters," *IEEE Microw. Wireless Compon. Lett.*, vol. 20, no. 12, pp. 669–671, Dec. 2010.
- [6] E. Naglich, J. Lee, D. Peroulis, and W. Chappell, "A tunable bandpass-to-bandstop reconfigurable filter with independent bandwidths and tunable response shape," *IEEE Trans. Microw. Theory Tech.*, vol. 58, no. 12, pp. 3370–3379, Dec. 2010.
- [7] E. Naglich, J. Lee, D. Peroulis, and W. Chappell, "Switchless tunable bandstop-to-all-pass reconfigurable filter," *IEEE Trans. Microw. Theory Tech.*, vol. 60, no. 5, pp. 1258–1265, May 2012.
- [8] S. Amari and U. Rosenbreg, "New building blocks for modular design of elliptic and self-equalized filters," *IEEE Trans. Microw. Theory Tech.*, vol. 52, no. 2, pp. 721–736, Feb. 2004.
- [9] E. Naglich, J. Lee, D. Peroulis, and W. Chappell, "Extended passband bandstop filter cascade with continuous 0.85–6.6-GHz coverage," *IEEE Trans. Microw. Theory Tech.*, vol. 60, no. 1, pp. 21–30, Jan. 2012.
- [10] J.-S. Hong and M. J. Lancaster, *Microstrip Filters for RF/Microwave Applications*, 1st. ed. New York: Wiley-Interscience, 2001.